Tough ion gels composed of coordinatively crosslinked polymer networks using ZIF-8 nanoparticles as multifunctional crosslinkers

Kamio, Eiji
Minakata, Masayuki
Nakamura, Hinako
Matsuoka, Atsushi
Matsuyama, Hideto

(Citation)
Soft Matter,18(25):4725-4736

(Issue Date)
2022-07-07

(Resource Type)
journal article

(Version)
Accepted Manuscript

ARTICLE

Tough ion gels composed of coordinatively crosslinked polymer networks using ZIF-8 nanoparticles as multifunctional crosslinkers

Received 00th January 20xx,
Accepted 00th January 20xx

DOI: 10.1039/x0xx00000x

Eiji Kamio,*[a,b,c] Masayuki Minakata,[a,b] Hinako Nakamura,[a,b] Atsushi Matsuoka,[a,b] and Hideto Matsuyama*[a,b]

Constructing crosslinked polymer networks via reversible interactions is a promising approach to recover the mechanical strength of damaged gels. In addition, by designing effective reversible crosslinks, the mechanical strength of the gel can be enhanced through energy dissipation based on the destruction of the crosslinks by an applied force. In this study, we introduced zeolitic imidazole framework-8 nanoparticles (ZIF-8 NPs), which acted as multifunctional crosslinkers, to provide multipoint coordination bonding with a poly(N,N-dimethylacrylamide)-based polymer network in a gel containing an ionic liquid. The mechanical strength of the gel increased with an increase in the content of ZIF-8 NPs up to 6 wt.%. It was confirmed that the energy loaded onto the gel was dissipated through the desorption of the polymer network from the surface of the ZIF-8 NPs. Owing to the reversible destruction and reconstruction of the coordinative crosslinking between the polymer network and ZIF-8 NPs, the mechanical strength of the damaged gel was almost fully recovered through annealing.

Introduction

Ionic liquids (ILs) are room-temperature molten salts with unique features, such as negligible vapor pressure, high ionic conductivity, non-flammability, high thermal/chemical/electrochemical stabilities, excellent CO_2 solubility, and versatile molecular structural design. Varying the design of the molecular structure and selection of cations and anions, various ILs have been developed as suitable materials for electrochemical devices, such as soft actuators, supercapacitors, lithium secondary batteries, fuel cells, and electric double-layer transistors.[1-7] ILs have also attracted significant attention as excellent separation media for CO_2, volatile organic compounds, bioactive components, metal ions, etc.[8-17] During practical applications, it is desirable to use ILs as solid-like materials, while maintaining their attractive properties. In this regard, a variety of strategies have been proposed to solidify ILs, such as the impregnation of an IL in a porous support material, polymerization of an IL-based monomer, and gelation of an IL. Among the developed IL-based solid materials, IL-based gels, termed 'ion gels,' have attracted considerable attention.[18, 19] Recently, ion gels with high mechanical strengths have been developed. The excellent mechanical strength of the ion gel enables the increase of the IL content in the gel, while maintaining a sufficient mechanical strength for practical applications. Because ion gels with high mechanical strengths are mainly composed of an IL, they not only maintain the unique intrinsic properties of ILs but also satisfy the requirements of high levels of safety, durability (even at elevated temperatures), ionic conductivity, and solute diffusivity.

To date, various methods have been proposed to fabricate ion gels with high mechanical strengths. Most ion gels are fabricated by designing a unique gel network structure. For example, tetra-arm poly(ethylene glycol) (tetra-PEG) ion gels possess a uniformly developed homogeneous gel network that can disperse the loaded energy to provide a high mechanical strength.[20, 21] Ion gels featuring a network formed by an ABA-type triblock copolymer with an IL-philic mid-block and IL-phobic crosslinkable end-blocks also demonstrate high mechanical strengths owing to improved energy dispersion.[22] Another example is the tough ion gel having a characteristic interpenetrating polymer network (IPN), which is termed as double network (DN) ion gel.[23-27] The toughening mechanism of the DN ion gels involves energy dissipation by the destruction of the brittle first network. These ion gels comprise a polymer network that is crosslinked by covalent bonds. Therefore, once the gel network is broken, the mechanical strength of the ion gels cannot be recovered. Recently, high-mechanical-strength ion gels, with characteristic networks formed via weak physical interactions, have been developed. Tamate *et al.* developed a high-mechanical-strength ion gel possessing a diblock polymer consisting of a polystyrene block that can aggregate in an IL to form a crosslinking point and a poly(dimetylacrylamide-*r*-acrylic acid) block that can form a weakly crosslinked network via

[a] *Department of Chemical Science and Engineering, Kobe University, 1-1 Rokkodai-cho, Nada-ku, Kobe, Hyogo 657-8501, Japan. Email: e-kamio@people.kobe-u.ac.jp (E.K.), matuyama@kobe-u.ac.jp (H.M.)*
[b] *Research Center for Membrane and Film Technology, Kobe University, 1-1 Rokkodai-cho, Nada-ku, Kobe, Hyogo 657-8501, Japan.*
[c] *Center for Environmental Management, Kobe University, 1-1 Rokkodai-cho, Nada-ku, Kobe, Hyogo 657-8501, Japan.*
Electronic Supplementary Information (ESI) available: [Synthesis of polymer network precursors, Synthesis scheme and size of ZIF-8 NPs, Characterization of ZIF-8 NPs in polymer/IL solution and ion gel samples, Mechanical propersy of the ion gel samples prepared using different size of ZIF-8 NPs]. See DOI: 10.1039/x0xx00000x

hydrogen bonding.[28] Ueki et al. developed a high-mechanical-strength ion gel with self-healing properties by forming a gel network using a photo-responsible azobenzene containing an ABA-type triblock copolymer.[29, 30] Weng *et al.* fabricated an ion gel with a high mechanical strength using an IPN consisting of polyvinyl alcohol (PVA), which forms a crystal structure in an IL, and polyvinylpyrrolidone (PVP), which forms a weakly crosslinked network with PVA via hydrogen bonding.[31] Because these ion gels had a gel network crosslinked by weak hydrogen bonds, they also had excellent mechanical strength owing to improved energy dissipation along with the destruction of the weak crosslinking structure. In addition, hydrogen bond-based crosslinking enabled the reversible destruction and reconstruction of the network and provided excellent self-repairing properties to the ion gels. The other tough ion gels, with a gel network formed via physical bonding, are the inorganic/organic DN and micro-double-network (μ-DN) ion gels having interpenetrating inorganic/organic networks.[32-34] The inorganic network of these ion gels was formed with silica nanoparticles (NPs), which were aggregated in a network-like structure via hydrogen bonding and van der Waals interactions. Because of the physical bonding of the network, the ruptured inorganic network could be repaired through annealing. Therefore, the inorganic/organic DN and μ-DN ion gels exhibited not only high mechanical strengths but also mechanical-strength-recovery properties.

The formation of weak crosslinks is a promising strategy for the development of ion gels with mechanical-strength-recovery properties. Weak crosslinking points can also be formed through interactions other than hydrogen bonding. In hydrogel systems, various weak crosslinks via electrostatic interactions, coordination bonds, π–π interactions, hydrophobic interactions, and host-guest interactions have been used, in addition to hydrogen bonds.[35] Coordination bonds, π–π interactions, hydrophobic interactions, and host–guest interactions might be used to crosslink the network in an ion gel. For example, in the ion gel prepared by Tamate *et al.*, polystyrene blocks, with a low affinity for the IL, aggregated to form crosslinking points based on the interaction between the polystyrene blocks.[28] The fabrication of ion gels utilizing the self-assembly of IL-phobic blocks was reported in several papers.[19, 22] In recent years, it was reported that high-mechanical-strength ion gels with self-healing properties could be fabricated by crosslinking the polymer networks through coordination bonds. For instance, Zhang *et al.* developed a high-stretching ion gel with self-healing properties using poly(acrylic acid)-coated Fe_3O_4 NPs as the crosslinking points via coordination bonding.[36] Zhu *et al.* also used Fe_3O_4 NPs as crosslinking points with coordination bonding to prepare a self-healing ion gel.[37] However, to the best of our knowledge, only Fe_3O_4 NPs have been reported as crosslinkers to form coordination bonds with the polymer network of ion gels. The utilization of coordination bonds to crosslink the polymer network of the ion gel and selection of the appropriate functional group(s) in the polymer network that would form coordination bonds with metal species could enable us to control the mechanical strength of the ion gel.

Recently, metal-organic frameworks (MOFs) have attracted significant attention owing to their outstanding structural, chemical, and functional diversities. MOF NPs can be easily prepared[38-40] and possess coordinatively unsaturated metal sites on their surface.[41-45] Therefore, we considered MOF NPs as multifunctional crosslinkers, which can provide multiple crosslinking points with the polymer networks in an ion gel.

In this study, we fabricated a novel ion gel, with a high mechanical strength, using NPs of zeolitic imidazole framework-8 (ZIF-8)—a type of MOF—as a multifunctional crosslinker with coordinative properties. The developed ion gel has a composite network of ZIF-8 nanoparticles and loosely crosslinked poly(*N,N*-dimethylacrylamide-*co*-*N*-succinimidyl acrylate) (poly(DMAAm-*co*-NSA). As the design criteria of the polymer network, the DMAAm unit was used as the coordinatively crosslinkable part with the ZIF-8 NPs, and the NSA unit was introduced to form three dimensional network by the chemical crosslinking between NSA groups. We investigated the toughening mechanism of the ion gel with ZIF-8 NPs based on the energy dissipation effect caused by the formation and destruction of the coordination bonds between the carbonyl group of the polymer networks and ZIF-8 NPs. Furthermore, we demonstrated the reversible recovery of the mechanical strength of the ion gels with ZIF-8 NPs.

Results and discussion

Interaction between ZIF-8 NPs and poly(*N,N*-dimetylacrylamide) (PDMAAm) in 1-butyl-3-methylimidazolium bis(trifluoromethyl-sulfonyl)imide ([Bmim][Tf_2N])

Because ZIF-8 NPs have coordinatively unsaturated metal sites, polymers with functional groups that can donate a lone pair of electrons to a metal site could form a coordination bond with the coordinatively unsaturated metal sites on the surface of the ZIF-8 NPs. In a preliminary evaluation, the formation of coordination bonds between the PDMAAm chains and Zn(II) in the IL was confirmed using FT-IR spectroscopy. In this investigation, to confirm the formation of a coordination bond between the carbonyl group (C=O) of PDMAAm and Zn(II), a PDMAAm homopolymer was used. Figure S1 shows the FT-IR spectra of the amide I band, which is mainly due to the C=O stretching vibration of the PDMAAm/[Bmim][Tf_2N] solutions with and without $Zn(NO_3)_2{\cdot}6H_2O$. For the solution without $Zn(NO_3)_2{\cdot}6H_2O$, the C=O stretching band of the amide group of *N,N*-dimetylacrylamide (DMAAm) is observed at 1639 cm^{-1}. In contrast, a new C=O stretching band for the DMAAm units is observed at a lower wavenumber (approximately 1605 cm^{-1}). When the amide C=O group interacts with another molecule, a new peak appears at wavenumbers lower than 1639 cm^{-1}.[28, 46] In addition, as shown in Figure S1(c-e), the intensity of the new peak increases with the increasing concentration of $Zn(NO_3)_2{\cdot}6H_2O$. Therefore, the observed new peak is due to the formation of a coordination bond between the DMAAm unit and Zn(II) in the IL. From these results, it can be expected that when ZIF-8 NPs and PDMAAm coexist in [Bmim][Tf_2N], several coordination bonds would be formed between the ZIF-8 NPs

and PDMAAm. Accordingly, the ZIF-8 NPs could act as a multifunctional crosslinker to toughen an ion gel composed of [Bmim][Tf_2N] and the PDMAAm network.

To confirm the formation of a coordination bond between the ZIF-8 NPs and PDMAAm, we prepared a suspension of the ZIF-8 NPs in [Bmim][Tf_2N] by dissolving PDMAAm and characterized it. A suspension of the ZIF-8 NPs was prepared as follows: First, ZIF-8 NPs were added to the PDMAAm solution dissolved in [Bmim][Tf_2N]/ethanol and were dispersed via vortex mixing and ultrasonication. The suspension was poured into a mold, and ethanol was completely evaporated by drying. Photographs of the ZIF-8 NP dispersion in IL/ethanol mixtures with and without PDMAAm are shown in Figure S2(a) and (b), respectively. In both figures, the photographs of the dispersions after ethanol removal were also shown. As clearly demonstrated in Figure S2(a), the color of the suspension considerably changes from opaque white to transparent owing to the removal of ethanol. Notably, the transparency significantly increases when PDMAAm coexists in the suspension. As shown in Figure S2(b), the color of the ZIF-8 NP suspension in [Bmim][Tf_2N] without PDMAAm does not change significantly after ethanol removal. These results indicate that the size of the ZIF-8 NP aggregates decreases when the ZIF-8 NPs and PDMAAm coexisted in [Bmim][Tf_2N]. The ZIF-8 NPs in [Bmim][Tf_2N] with PDMAAm are smaller than those in the suspension without PDMAAm (Figure S3). This means that PDMAAm strongly contributes to the dispersion of ZIF-8 NPs in [Bmim][Tf_2N]. In other words, PDMAAm acts as a dispersion stabilizer for ZIF-8 NPs. This indicates that PDMAAm is adsorbed on the surface of the ZIF-8 NPs in [Bmim][Tf_2N].

To confirm the adsorption of PDMAAm on ZIF-8 NPs, we conducted an adsorption experiment. Figure 1 indicates the relationship between the molar ratio of DMAAm-to-[Bmim][Tf_2N] and the ZIF-8 NP content in the suspension. As shown in this figure, the DMAAm unit/[Bmim][Tf_2N] ratio in the solution after the adsorption experiment monotonically decreases with an increase in the content of ZIF-8 NPs. If Zn ion from the degraded ZIF-8 mainly forms coordination bond with PDMAAm, the concentration of PDMAAm in the solution will be hardly decreased after the adsorption test. However, the result shown in Figure 1 indicated the clear decrease of the PDMAAm concentration. This decrease is due to the removal of PDMAAm from the solution; that is, it is considered that PDMAAm is adsorbed onto the ZIF-8 NPs and removed from the solution along with the ZIF-8 NPs. Therefore, in the ZIF-8 NP suspension, it is considered that it was ZIF-8 NPs, not released Zn ion, that crosslinked PDMAAm.

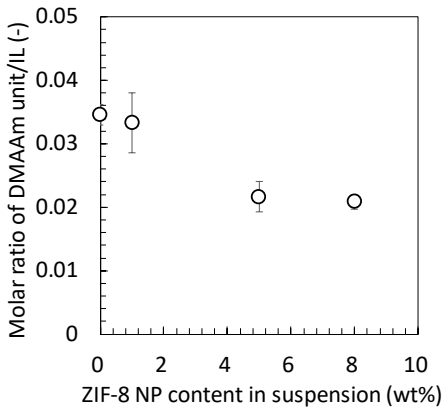

Figure 1 Relationship between the DMAAm unit/[Bmim][Tf_2N] molar ratio in the supernatant after adsorption experiment and the concentration of added ZIF-8 NPs.

In the case of another tough ion gel composed of silica NPs and PDMAAm, named μ-DN ion gel, which we developed previously, the trend observed was completely opposite; that is, the DMAAm unit/[Bmim][Tf_2N] ratio increased with an increase in the content of silica NPs.[47] This means that in the case of the μ-DN ion gel, PDMAAm was not adsorbed on the silica NPs, but rather [Bmim][Tf_2N] was adsorbed. The opposite trend is likely due to the different interactions that PDMAAm has with ZIF-8 and silica NPs. The interaction between the PDMAAm and ZIF-8 NPs in [Bmim][Tf_2N] is stronger than that between the PDMAAm and silica NPs. This stronger interaction could be due to the formation of coordination bonds. To confirm the formation of coordination bonds, the interaction between PDMAAm and ZIF-8 NPs was determined using FT-IR measurements. As mentioned previously, the C=O group in PDMAAm formed a coordination bond with Zn(II) in [Bmim][Tf_2N], and an FT-IR absorbance peak at approximately 1605 cm^{-1} appeared when $Zn(NO_3)_2{\cdot}6H_2O$ was added to the solution (Figure S1). Similarly, in the case of the ZIF-8 NPs, it was expected that a new peak would appear if the C=O group also formed a coordination bond with the coordinatively unsaturated Zn(II) on the surface of the ZIF-8 NPs in [Bmim][Tf_2N]. Therefore, to confirm the formation of a coordination bond between the C=O group in PDMAAm and coordinatively unsaturated Zn(II) on the surface of the ZIF-8 NPs, FT-IR spectra were recorded for the ZIF-8 NP suspensions with different concentrations of ZIF-8 NPs in [Bmim][Tf_2N], while keeping the concentration of PDMAAm constant. As shown in Figure 2, the intensity of the peak at 1639 cm^{-1}, which is related to the stretching vibration of the C=O group, decreases, and a new peak appears at approximately 1605 cm^{-1} when the content of the ZIF-8 NPs in the suspension increases. This trend is the same as that observed for the mixture of [Bmim][Tf_2N], PDMAAm, and $Zn(NO_3)_2{\cdot}6H_2O$ (Figure S1). However, when compared with that of the μ-DN ion gel composed of PDMAAm and silica NPs, the trend observed in this study is completely different. In the case of the μ-DN ion gel, the wavenumber of the peak associated with the stretching vibration of the C=O group did not decrease, and no new peak appeared as the content of the silica NPs increased.[47] This was because PDMAAm did not adsorb on the silica NPs. In other words, PDMAAm has strong interactions with the ZIF-8 NPs in [Bmim][Tf_2N]. Therefore, the appearance of the new peak in Figure 2 demonstrates that PDMAAm forms a coordination bond with the coordinatively unsaturated Zn(II) on the ZIF-8 NPs.

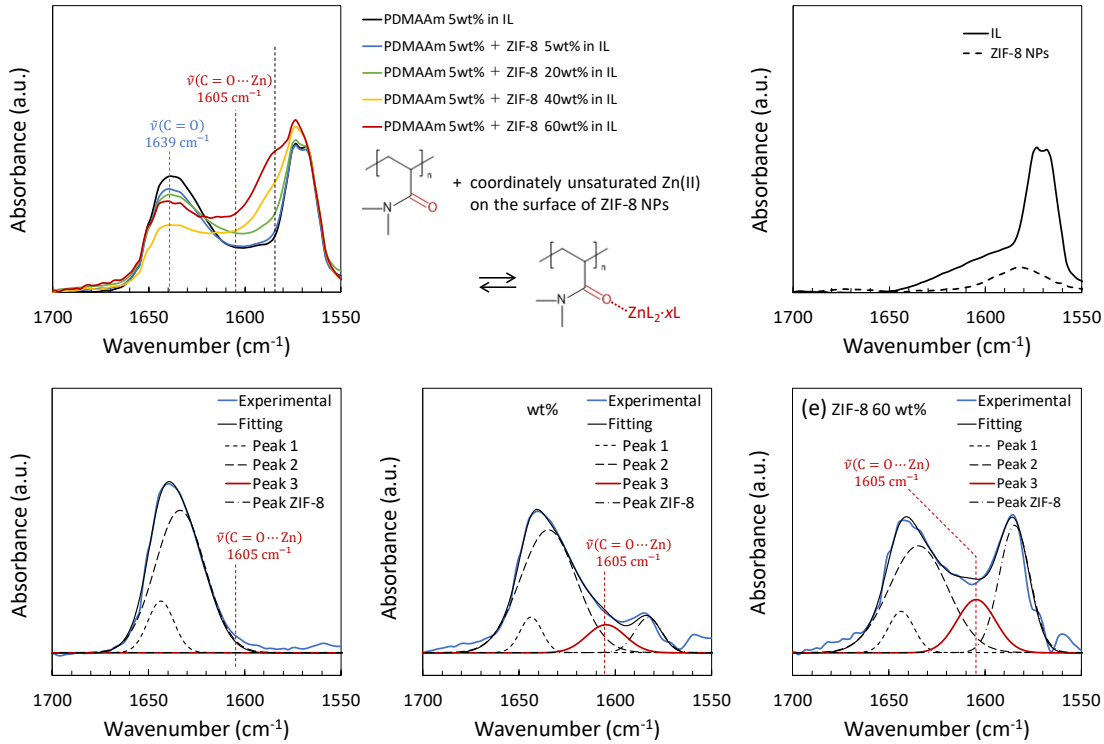

Figure 2 Normalized FT-IR spectra of ZIF-8 NP/PDMAAm/[Bmim][Tf_2N] suspensions. (a) ZIF-8 NP concentration effect on the FT-IR spectra of the ZIF-8 NP/PDMAAm/[Bmim][Tf_2N] suspensions, (b) FT-IR spectra of [Bmim][Tf_2N] and ZIF-8 NPs, (c) baseline-subtracted amide I band of the PDMAAm/[Bmim][Tf_2N] solution without ZIF-8 NPs, (d, e) baseline-subtracted amide I band of the ZIF-8 NP/PDMAAm/[Bmim][Tf_2N] solutions with different concentrations of the ZIF-8 NPs in [Bmim][Tf_2N]. The Peaks 1 and 2 shown in (c) - (e) could be assigned to the carbonyl groups that formed no hydrogen bonds and the carbonyl groups that are bounded to water molecule or IL molecule through a hydrogen bond, respectively.[46, 48] The Peak 3 in these figures is the carbonyl groups that are bounded to coordinatively unsaturated zinc on the surface of ZIF-8 NPs.

From the results shown in Figures 1 and 2, it can be concluded that PDMAAm is adsorbed on the surface of the ZIF-8 NPs because of the formation of a coordination bond between PDMAAm and the ZIF-8 NPs in [Bmim][Tf_2N]. Because ZIF-8 NPs have many coordinatively unsaturated Zn(II) on the surface,[41-45] the ZIF-8 NPs probably act as multifunctional crosslinkers of the PDMAAm network and toughen the ion gel containing [Bmim][Tf_2N].

Mechanical strength of an ion gel containing ZIF-8 NPs

The ZIF-8 NP ion gel was fabricated using poly(DMAAm-*co*-NSA) with 2 mol% of NSA as the chemical crosslinking group because it was not prepared when the polymer network was not chemically crosslinked. The ZIF-8 NP ion gel composed of 80 wt.% [Bmim][Tf_2N], 15 wt.% poly(DMAAm-*co*-NSA), and 5 wt.% ZIF-8 NPs is shown in Figure 3. A transparent, self-standing ion gel is formed. The transparency of the ion gel indicates that the ZIF-8 NPs are well-dispersed as very small aggregates in the ion gel. In terms of transparency, similar to the phenomenon observed for the ZIF-8 NP suspension (Figure S2), the color of the ion gel changed from opaque white to transparent when ethanol was removed from the gel. This possibly means that the ZIF-8 NPs exist in the ion gel in the same state as those in the PDMAAm/[Bmim][Tf_2N] solution; that is, the ZIF-8 NPs may have adsorbed the PDMAAm segment of the polymer network in the ion gel. Although it was impossible to measure the size of the ZIF-8 NP aggregates in the ZIF-8 NP ion gel, it was confirmed using XRD measurements that the ZIF-8 NPs exist in the ion gel and maintain their crystalline structure (Figure S4). Therefore, it is probable that the ZIF-8 NPs act as multifunctional crosslinkers that toughen the ion gel.

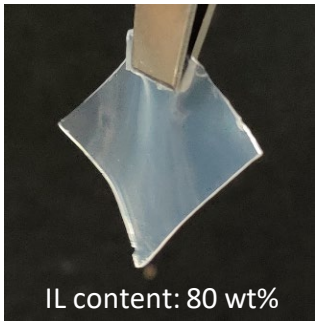

Figure 3 Prepared ion gel composed of 20 wt.% of the ZIF-8/poly(DMAAm-*co*-NSA) composite network and 80 wt.% of [Bmim][Tf_2N].

To investigate the mechanical strength of the ZIF-8 NP ion gels, uniaxial stretching experiments were conducted on the ion gels with different contents of the ZIF-8 NPs. The results are shown in Figure 4. The stress-strain curves of the ion gels with different ZIF-8 NP contents are shown in Figure 4(a). The results

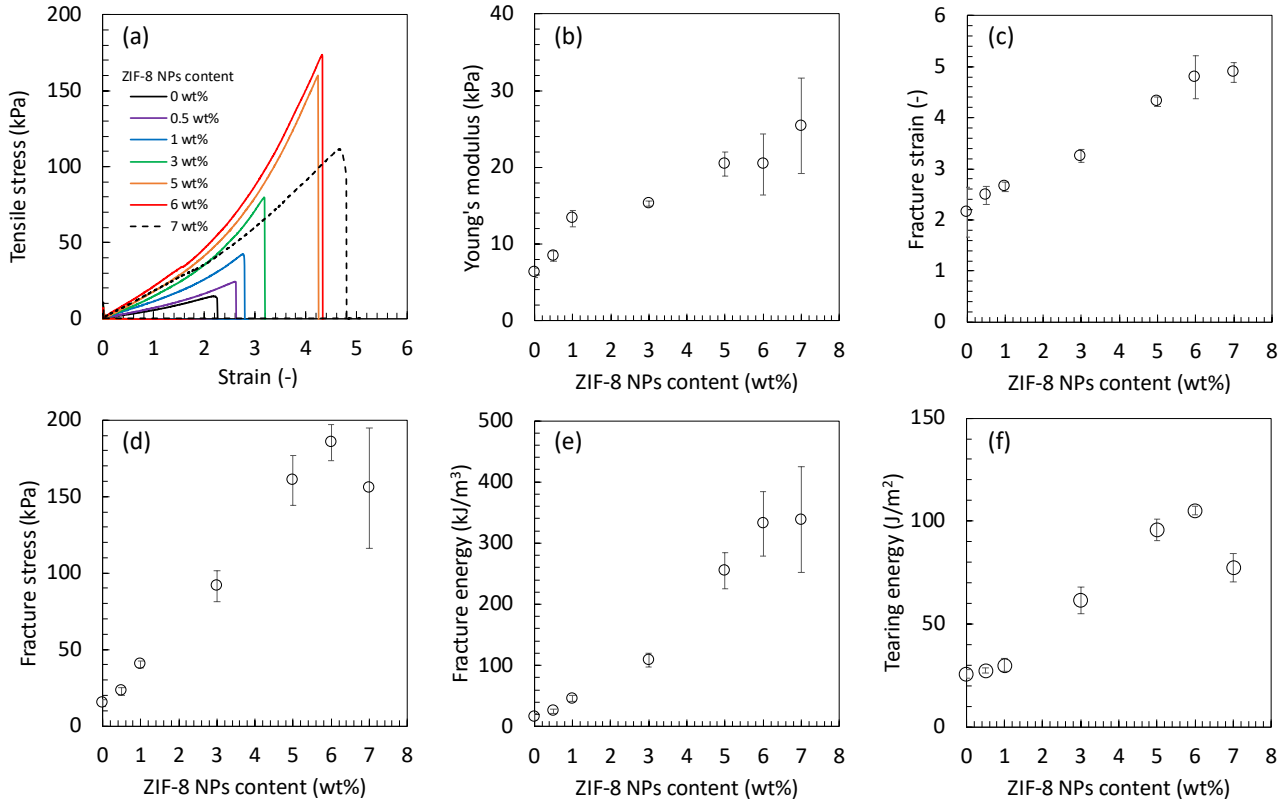

Figure 4 Mechanical properties of ZIF-8 NP ion gels composed of [Bmim][Tf_2N] (80 wt.%) and the ZIF-8 NP/PDMAAm composite network (20 wt.%) with various ZIF-8 compositions. (a) Stress-strain curves of ZIF-8 NP ion gels containing various concentrations of ZIF-8 NPs, (b) Young's modulus, (c) fracture strain, (d) fracture stress, (e), fracture energy, and (f) tearing energy.

for the PDMAAm SN ion gel composed of 80 wt.% [Bmim][Tf_2N] and 20 wt.% poly(DMAAm-*co*-NSA) network (i.e., 0 wt.% ZIF-8 NPs) are also shown. The mechanical strength of the ZIF-8 NP ion gel is higher than that of the PDMAAm SN ion gel. In addition, the mechanical strength of the ZIF-8 NP ion gels increases with an increase in the ZIF-8 NP content up to 6 wt.%. These resultsclearly indicate that the ZIF-8 NPs enhance the mechanical strength of the ion gel. Considering the adsorption of PDMAAm onto the ZIF-8 NPs, it is proposed that the ZIF-8 NPs act as multifunctional crosslinkers that increase the mechanical strength of the ion gel. However, when the ZIF-8 NP content is 7 wt.%, the mechanical strength decreases. This could be due to the lack of a polymer network capable of sustaining the large number of ZIF-8 NPs. Therefore, the optimal ZIF-8 NP content to toughen the ion gel is 6 wt.%.

The mechanical properties, such as Young's modulus, fracture strain, fracture stress, fracture energy, and tearing energy, are summarized in Figures 4(b)–(f), respectively. The Young's modulus increases with an increase in the ZIF-8 NP content. This increase in the Young's modulus can be explained by the possibility that ZIF-8 NPs act as multifunctional crosslinkers. If the ZIF-8 NPs act as multifunctional crosslinkers, the number of crosslinking points between the polymer network and ZIF-8 NPs increases with an increase in the ZIF-8 NP content. Therefore, the load is sustained by several polymer chains crosslinked by ZIF-8 NPs. As a result, the Young's modulus of the ZIF-8 NP ion gel increases with an increase in the ZIF-8 NP content. In addition, the increase in the fracture strain can be explained considering the contribution of ZIF-8 NPs as multifunctional crosslinkers. Therefore, even though some of the polymer networks break, the remaining ones sustain the load and prevent the macro-destruction of the ion gel. Owing to the increase in the Young's modulus and fracture strain, the fracture stress and fracture energy of the ZIF-8 NP ion gel also increases with an increase in the ZIF-8 NP content. In addition, as shown in Figure 4(f), the tearing energy of the ZIF-8 ion gel increases with an increase in the ZIF-8 NP content. Therefore, the ZIF-8 NPs in the ion gel contribute to the toughening of the ion gel.

Toughening mechanism of an ion gel containing ZIF-8 NPs

To confirm the toughening mechanism of the ZIF-8 NP ion gels, a cyclic tensile stress loading–unloading experiment was conducted. The results shown in Figure 5 indicate a clear hysteresis loop in the cyclic stress-strain curves and softening behavior of the ZIF-8 NP ion gel upon the application of force. The softening behavior is due to the structural change of the gel network caused by the force applied to the gel. Therefore, the hysteresis loop indicates that the energy loaded onto the ZIF-8 ion gel dissipates when the ZIF-8/poly(DMAAm-co-NSA) composite network is deformed or destroyed. This energy

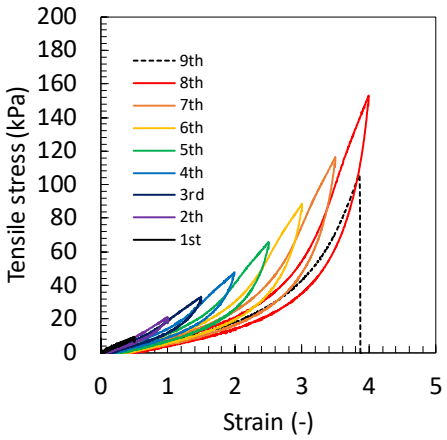

Figure 5 Cyclic tensile stress-strain curves of the ZIF-8 NP ion gel prepared using ZIF-8 NPs synthesized at 333 K. Composition of [Bmim][Tf_2N], poly(DMAAm-*co*-NSA), and ZIF-8 NP in the ion gel were 80, 15, and 5 wt.%, respectively.

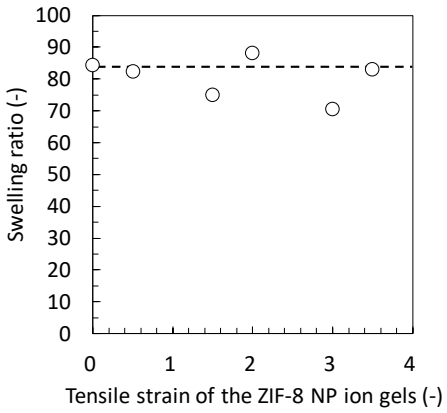

Figure 6 Swelling ratio of the polymer network skeleton of the ZIF-8 NP ion gels stretched at certain tensile strains. The polymer network skeletons were obtained from the stretched ion gels by removing [Bmim][Tf_2N] using ethanol followed by dissolving ZIF-8 NPs using NaOH aqueous solution.

dissipation is the main reason for the increased mechanical strength of the ZIF-8 NP ion gel.

Subsequently, we considered the cause of the energy dissipation in the ZIF-8 NP ion gels. There are three main possible causes for the energy dissipation in an ion gel with a composite network composed of NPs and a polymer network.

The first possibility is the destruction of the NP aggregates in the ion gel, as was the case for the inorganic/organic DN and μ-DN ion gels.[33, 34, 49] In this case, the loaded energy dissipates when the NP aggregates are disassembled by the load applied to the gel. The interaction between the NPs forming the aggregates is dependent on their size. Therefore, the amount of energy dissipated by the destruction of the NP aggregates and the mechanical strength of the ion gel depend on the size of the NPs. In fact, it was reported that the mechanical strength of the inorganic/organic μ-DN ion gels was strongly dependent on the primary particle size of the silica NPs.[33] In addition, because the number of NPs forming the aggregate in the ion gel decreases when the primary particle diameter is increased, the dissipated energy will decrease with an increase in the primary particle diameter if the destruction of the aggregates of the NPs is the cause of the energy dissipation. In the μ-DN ion gel, the dissipated energy decreased with an increase in the primary particle diameter of the silica NPs.[33] Therefore, the evaluation of the effect of the primary particle size on the mechanical strength of ZIF-8 ion gels can determine whether the destruction of the NP aggregates was the cause of the energy dissipation.

ZIF-8 NPs of different sizes were prepared by changing the temperature of the ZIF-8 NP synthesis. The transmission electron microscopy (TEM) images of the ZIF-8 NPs used for the preparation of ZIF-8 NP ion gels are shown in Figure S5. The primary particle diameter varies between 17.5 and 120 nm. Figure S6(a) shows the stress-strain curves of the ZIF-8 NP ion gels prepared using ZIF-8 NPs with different primary particle sizes. The mechanical strength of the ZIF-8 NP ion gel is not dependent on the primary particle size of the ZIF-8 NPs. In addition, the results of the cyclic stress loading-unloading experiment involving the ZIF-8 NP ion gel shows clear hysteresis (Figure S6(b-d)). It is confirmed that the dissipated energies in the ZIF-8 NP ion gels prepared using different sizes of the ZIF-8 NPs are almost identical. Therefore, these results indicate that the destruction of ZIF-8 NP aggregates in the gel was not the cause of energy dissipation.

The second possible cause for the energy dissipation is the destruction of the polymer network in the gel. Even if the chemical bond of the polymer network is destroyed, the ZIF-8 NPs might crosslink the destroyed polymer networks and prevent the macro-destruction of the ion gel. However, if this second possibility was the cause of the energy dissipation in the ZIF-8 NP ion gel, some parts of the polymer network would be broken after the elongation of the gel. As a result, when the polymer network skeleton without the ZIF-8 NPs obtained from the ZIF-8 NP ion gel after elongation is immersed in water, it should swell more than the polymer network skeleton of the fresh ZIF-8 NP ion gel. Therefore, we conducted a swelling experiment on the polymer network skeleton of the ZIF-8 NP ion gels after elongation to clarify whether the destruction of the polymer network was the cause of the energy dissipation. The results of the swelling experiments are shown in Figure 6. The swelling ratio of the polymer network skeletons of the ZIF-8 NP ion gel in pure water do not exhibit a clear dependence on the tensile strain of the ZIF-8 NP ion gels. Notably, the swelling ratio of most of the polymer network skeleton of the ZIF-8 NP ion gels after elongation is lower than that of the original ZIF-8 NP ion gel (the tensile strain of the ZIF-8 NP ion gel is 0). This result indicates that the polymer network of the ZIF-8 NP ion gel is not destroyed after elongation by at least 3.5% of the tensile strain. Therefore, the destruction of the polymer network in the ZIF-8 NP ion gel was not the cause of the energy dissipation.

The third possibility is the desorption of the polymer network from the NP aggregates. As mentioned previously, the PDMAAm network can adsorb onto the ZIF-8 NPs. It is possible to dissipate the energy loaded onto the ZIF-8 NP ion gel via the desorption of PDMAAm from the ZIF-8 NPs. Therefore, it is proposed that the toughening mechanism of the ZIF-8 NP ion

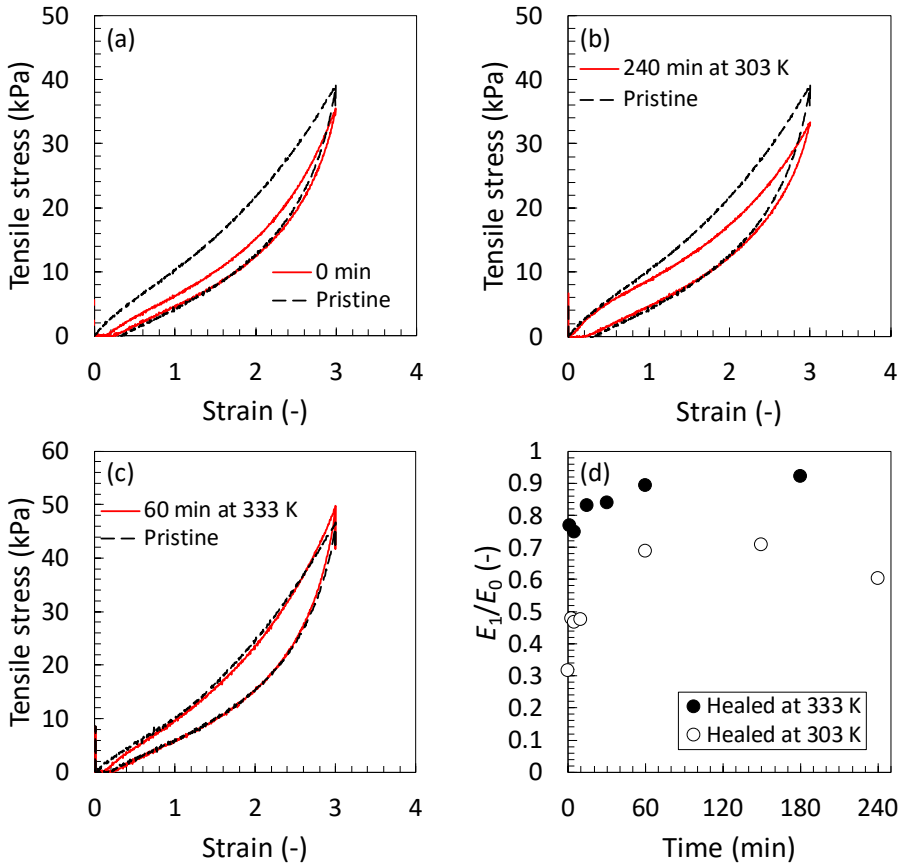

Figure 7 Recovery of the mechanical strength of the ZIF-8 NP ion gel stretched up to a strain of 3.0. ZIF-8 NP ion gel composed of 80 wt.% of [Bmim][Tf_2N], 15 wt.% of poly(DMAAm-*co*-NSA), and 5 wt.% of ZIF-8 NPs was used. The ZIF-8 NPs prepared at 333 K was used to prepare the ion gel. Time and temperature for the network recovery: (a) 0 min, (b) 240 min at 303 K, and (c) 60 min at 333 K. (d) Time courses of the recovery ratios of the mechanical strength.

gel is through the energy dissipation caused by the desorption of the poly(DMAAm-co-NSA) network from the ZIF-8 NPs.

Recovery of mechanical properties of the ZIF-8 NP ion gels

From the results mentioned above, it can be concluded that the ZIF-8 NPs act as multifunctional crosslinkers that toughen theZIF-8 NP ion gels. The crosslinking between the poly(DMAAm-*co*-NSA) network and ZIF-8 NPs is formed through the coordination bond between the C=O group of PDMAAm and the coordinatively unsaturated Zn(II) on the surface of ZIF-8 NPs. Because of the reversible nature of the coordination bond, it was expected that the composite network that was destroyed through the application of force would be recovered by the reconstruction of the coordination bonds. Therefore, we conducted an experiment to determine the recovery of the mechanical strength of the ZIF-8 NP ion gel that had been softened by stretching. Recovery experiments were performed at 303 and 333 K. The samples with the recovered networks were prepared by keeping the pre-stretched ZIF-8 NP ion gels in a thermostat oven at 303 and 333 K for a certain period of time. The stress-strain curves of the pristine ZIF-8 NP ion gel before stretching and that of the sample with the recovered network are shown in Figure 7. The mechanical strength of the softened ZIF-8 NP ion gel is significantly improved. In this study, based on the results of the recovery experiment, we quantitatively evaluated the degree of coordination bond recovery by the ratio of the dissipated energy of the recovered ion gel sample, E_1, to that of the pristine sample, E_0. The time courses of the recovery ratios at 303 K and 333 K are shown in Figure 7(d). At high temperatures, the rate and degree of coordination bond recovery are fast and high, respectively. Notably, the mechanical strength of the ZIF-8 NP ion gel is almost fully recovered within 1 h when the temperature is 333 K, which is the same as the preparation temperature of the ZIF-8 NP ion gel. The network recovery properties of the ZIF-8 NP ion gels result from the reversible coordination bonds between the ZIF-8 NPs and the poly(DMAAm-*co*-NSA) network. This mechanism can be explained as follows: When a force is applied to the ZIF-8 NP ion gel, the poly(DMAAm-*co*-NSA) network is desorbed from the surface of the ZIF-8 NPs. When the applied force is unloaded, the shape of the ZIF-8 NP ion gel recovers owing to the elasticity of the polymer network. However, under ambient temperature conditions, the polymer network does not fully recover its original conformation because the ZIF-8 NPs cannot be packed in their original density. The small spaces among the ZIF-8 NPs result in the macro-deformation of the gel and restricts the

complete recovery of the coordination bond between the ZIF-8 NPs and polymer network. Therefore, at 303 K, the energy dissipation cannot be fully recovered, even after 240 min (Figure 7(b)), because of the small number of crosslinking points present after network recovery. However, when the ZIF-8 NP ion gel is maintained at 333 K after the first stretching, the mechanical strength rapidly recovers almost completely (Figure 7(c)). In this case, the coordination bonds between the ZIF-8 NPs and polymer network weaken at elevated temperatures. As a result, both the ZIF-8 NPs and polymer network become free from coordination bonds; the refolding of the polymer network is no longer restricted, and the packing of the composite network is recovered. When the ZIF-8 NP ion gel is cooled to the ambient temperature after annealing at 333 K, the coordination bond between the ZIF-8 NPs and polymer networks is recovered, and the toughness of the ZIF-8 NP ion gel is restored.

Conclusions

A tough ion gel composed of polymer networks that are coordinatively crosslinked with ZIF-8 NPs was developed. The polymer network used to fabricate the tough ion gel was poly(DMAAm-*co*-NSA), in which the DMAAm unit could form coordination bonds with coordinatively unsaturated Zn(II) on the surface of the ZIF-8 NPs, and the NSA unit was loosely crosslinked by a diamine unit. In the developed ion gel, the ZIF-8 NPs acted as multifunctional crosslinkers that toughen the ion gel. The toughening mechanism of the developed ion gel was based on energy dissipation, which was caused by the desorption of the polymer network from the surface of the ZIF-8 NPs. Because the polymer network was adsorbed on the surface of ZIF-8 NPs through a reversible coordination bond, the mechanical strength of the ion gel softened by the application of force could be recovered by reconstructing the coordination bond between the polymer network and ZIF-8 NPs. The recovery of mechanical strength of the ion gel could be accelerated via annealing and was almost fully recovered within 60 min at 333 K.

The findings of this proof-of-concept study demonstrate that ZIF-8 NPs can be used as a useful filler to toughen ion gels. We believe that the utilization of MOF NPs could open a new avenue for the development of novel tough and functional ion gels.

Experimental

Materials

For the synthesis of ZIF-8 NPs, 2-methylimidazole and zinc nitrate hexahydrate (98%), purchased from Sigma-Aldrich Co. and FUJIFILM Wako Pure Chemical Co., Ltd., respectively, were used as received. Methanol (FUJIFILM Wako Pure Chemical Co., Ltd.) was used as the solvent. *N,N*-dimethylacrylamide (DMAAm) and *N*-succinimidyl acrylate (NSA) were used as monomers for synthesizing the crosslinkable polymer, poly(*N,N*-dimethylacrylamide-*co*-*N*-succinimidyl acrylate) (poly(DMAAm-*co*-NSA)). They were purchased from Tokyo Chemical Industry Co., Ltd. DMAAm was used after removing the polymerization inhibitor by passing it through a column with activated alumina (FUJIFILM Wako Pure Chemical Co., Ltd.). For the synthesis of the crosslinkable polymer *via* reversible addition-fragmentation chain transfer (RAFT) polymerization, 2,2'-azobis(2,4-dimethylvaleronitrile) (FUJIFILM Wako Pure Chemical Co., Ltd.), 2-(dodecylthiocarbonothioylthio)-2-methylpropionic acid (Sigma-Aldrich Co.), and super-dehydrated 1,4-dioxane (FUJIFILM Wako Pure Chemical Co., Ltd.) were used as the radical initiator, chain transfer agent, and solvent, respectively. For the purification of the synthesized crosslinkable polymer *via* precipitation, tetrahydrofuran (THF) and n-hexane were used as good and poor solvents, respectively. They were purchased from FUJIFILM Wako Pure Chemical Co., Ltd. and used as received. To determine the molecular weight of the synthesized polymer using size-exclusion chromatography (SEC) analysis, high-performance liquid chromatography (HPLC)-grade THF (FUJIFILM Wako Pure Chemical Co.) was used as the solvent and mobile phase. Triethylamine (TEA, Tokyo Chemical Industry Co., Ltd.) was used as an amine additive for the SEC analysis. *Tert*-butylamine, *N*-tert-butylacrylamide, and *N*-hydroxysuccinimide were used to determine the molar ratio of NSA introduced in the crosslinkable polymer *via* proton nuclear magnetic resonance (^{1}H NMR) spectroscopy. These samples were purchased from Tokyo Chemical Industry Co., Ltd. For the ^{1}H NMR measurements, dimethyl sulfoxide-d_6 (d_6-DMSO, FUJIFILM Wako Pure Chemical Co.) was used as the solvent.

For preparing the ion gel, 1-butyl-3-methylimidazolium bis(trifluoromethylsulfonyl)imide ([Bmim][Tf_2N], Sigma–Aldrich Co.) was used as received. The polymer network of the ion gels was formed *via* the chemical crosslinking of the synthesized poly(DMAAm-*co*-NSA). For chemical crosslinking, diethylene glycol bis(3-aminopropyl)ether (DGBE, Tokyo Chemical Industry Co., Ltd.) was used as the crosslinker. Ethanol (FUJIFILM Wako Pure Chemical Co.) was used as the diluent for the ion gel precursor solution.

Synthesis and characterization of ZIF-8 NPs

Preparation of ZIF-8 NP suspension in methanol. ZIF-8 NPs were synthesized according to a previously reported procedure (Scheme S1).[50] First, solution A was prepared by dissolving 3.69 g (0.0124 mol) of $Zn(NO_3)_2{\cdot}6H_2O$ in 250 cm^3 of methanol. Solution B was prepared by dissolving 8.125 g (0.10 mol) of 2-methylimidazole in 250 cm^3 of methanol. Solution B was heated to a specific temperature with agitation at 500 rpm. Solution A was then added to Solution B upon reaching the targeted temperature. The mixture was continuously agitated at 500 rpm for 1 h at a specific temperature. After 1 h, ZIF-8 NPs were formed in solution. ZIF-8 NPs with different sizes were synthesized at 263, 273, 303, and 323 K. The synthesized ZIF-8 NPs were collected via centrifugation at 10,000 rpm for 30 min. To purify the obtained ZIF-8 NPs, a sufficient volume of methanol was added to the collected ZIF-8 NP slurry, and the suspension was vigorously agitated through vortex mixing for 1 min and centrifuged at 10,000 rpm for 30 min. This purification

process was repeated three times. Subsequently, a sufficient volume of methanol was added to the purified ZIF-8 NP slurry, and the ZIF-8 NPs were homogeneously dispersed via vortex mixing for 1 min, followed by ultrasonication for 1 h. The concentration of the ZIF-8 NPs in the suspension was determined as follows: Approximately 1 g of the ZIF-8 NP suspension was collected in a glass vial, and methanol was evaporated in a thermostat oven at 333 K for 12 h. The methanol was completely evaporated at 373 K for 1 h under vacuum, and the weight of the obtained dry ZIF-8 NPs was measured. The concentration of the ZIF-8 NPs in the starting suspension was determined from the weights of the suspension and dry ZIF-8 NPs. The obtained ZIF-8 suspension in methanol was stored in a glass vial at room temperature (298 K).

Measurement of the size of ZIF-8 NPs. The size of the synthesized ZIF-8 NPs was determined via transmission electron microscopy (TEM). A drop of the ZIF-8 NP suspension in methanol was added onto a copper mesh TEM grid. The TEM grid containing the suspension was dried in a desiccator under vacuum for 12 h at room temperature (298 K). TEM imaging was conducted using field-emission TEM (JEM-2100F, JEOL Ltd.). The acceleration voltage of the electron gun used for the imaging was 200 kV.

Synthesis of poly(N,N-dimethylacrylamide) (PDMAAm) and evaluation of its adsorption ability on ZIF-8 NPs

Synthesis of PDMAAm. To confirm the formation of a coordination bond between the carbonyl group (C=O) of PDMAAm and Zn(II), a PDMAAm homopolymer was used. PDMAAm was synthesized via RAFT polymerization. The details of the PDMAAm synthesis are provided in the Supporting Information. The molecular weight of the synthesized PDMAAm was determined using an SEC system with light scattering detectors (GPCmax, TDA305, triple detection model, with refractive index, right-angle light scattering, and low-angle light scattering detectors and viscometer, Malvern Panalytical Ltd.) and a column for the organic solvent system (Shodex LF-804, ID: 8.0 mm, length: 300 mm, Showa Denko K.K., Japan). THF containing 5 wt.% TEA at a flow rate of 1.0 cm^3/min was used as the mobile phase for the SEC analysis. The calculated weight-averaged molecular weight (M_w), number-averaged molecular weight (M_n), and polydispersity (M_w/M_n) were 146 kg/mol, 85 kg/mol, and 1.70, respectively.

Fourier-transform infrared (FT-IR) spectroscopy measurements. Coordination bond formation between Zn(II) and PDMAAm was confirmed by analyzing the spectral shift of the FT-IR band for the C=O group in PDMAAm. FT-IR spectra were measured using a Nicolet iS5 FT-IR spectrometer (Thermo Scientific Inc.).

As a preliminary experiment, coordination bond formation between $Zn(NO_3)_2{\cdot}6H_2O$ and PDMAAm in [Bmim][Tf_2N] was evaluated. First, 0.474 g of PDMAAm was dissolved in 3.0 g of ethanol, and then 9.0 g of [Bmim][Tf_2N] was dissolved in the solution. The solution was dried at 373 K for 12 h under vacuum to completely evaporate the ethanol. In 1.0 g of the obtained solution with 5.0 wt.% PDMAAm, a certain weight of $Zn(NO_3)_2{\cdot}6H_2O$ was dissolved. The concentrations of $Zn(NO_3)_2{\cdot}6H_2O$ in the solutions were 0, 0.1, 0.5, and 1.0 wt.%, respectively. The FT-IR spectra of the PDMAAm/[Bmim][Tf_2N] and $Zn(NO_3)_2{\cdot}6H_2O$/PDMAAm/[Bmim][Tf_2N] solutions were recorded, and the effect of the $Zn(NO_3)_2{\cdot}6H_2O$ concentration on the wavenumber shift of the C=O band was evaluated.

Additionally, coordination bond formation between the coordinatively unsaturated Zn(II) on the surface of ZIF-8 NPs and PDMAAm in [Bmim][Tf_2N] was evaluated. In this case, a certain weight of the ZIF-8 NP suspension in methanol was added to 1.0 g of the PDMAAm/[Bmim][Tf_2N] solution with 5.0 wt.% PDMAAm, which was prepared in the same manner as mentioned above. The ZIF-8 NP suspension in PDMAAm/methanol/[Bmim][Tf_2N] was dried at 373 K for 12 h under vacuum to completely evaporate methanol and consequently produce a ZIF-8 NP suspension in the PDMAAm/[Bmim][Tf_2N] solution. The concentrations of the ZIF-8 NPs in the suspensions were 5.0, 20.0, 40.0, and 60.0 wt.%, respectively. The FT-IR spectra of the PDMAAm/[Bmim][Tf_2N] solution and ZIF-8 NP suspensions were measured, and the effect of the ZIF-8 NP concentration on the FT-IR spectral shift of the C=O band was evaluated.

Evaluation of the adsorption ability of PDMAAm on ZIF-8 NPs. To evaluate the adsorption behavior of PDMAAm on ZIF-8 NPs, we conducted an adsorption experiment. The adsorption behavior could be evaluated through the composition change of PDMAAm in the PDMAAm/[Bmim][Tf_2N] solution before and after contact with the ZIF-8 NPs. A PDMAAm homopolymer was used for the adsorption experiment. First, 0.100 g of the synthesized PDMAAm and 9.9 g of [Bmim][Tf_2N] were dissolved stepwise in 2.0 g of ethanol, and the solution was subsequently dried at 373 K for 12 h under vacuum to completely evaporate the ethanol. In 1.0 g of the obtained 1.0 wt.% PDMAAm solution in [Bmim][Tf_2N], a certain weight of dry ZIF-8 NPs was added. The concentrations of the ZIF-8 NPs in the suspensions were 1.0, 5.0, and 8.0 wt.%, respectively. The suspension was stirred continuously using a magnetic stirrer for 6 h at room temperature (298 K). After 6 h, the ZIF-8 NPs were separated via centrifugation at 8000 rpm for 10 min. The supernatant was collected using a Pasteur pipette and filtered through a syringe filter with a pore size of 0.45 µm. The ^{1}H NMR spectrum of the obtained solution was recorded. From the integral ratio of the peaks corresponding to the N-$(CH_3)_2$ group of DMAAm and CH_3 group of [Bmim][Tf_2N], the molar ratio of PDMAAm-to-[Bmim][Tf_2N] in the solution was determined. From the molar ratios determined before and after contact with the ZIF-8 NPs, the composition variation of PDMAAm in the PDMAAm/[Bmim][Tf_2N] solution was determined.

Preparation and characterization of an ion gel composed of a PDMAAm network and ZIF-8 NPs (ZIF-8 NP ion gel)

Synthesis of the crosslinkable polymer (poly(DMAAm-co-NSA)). Poly(DMAAm-*co*-NSA) was used as the precursor of the polymer network of the ZIF-8 NP ion gel. It was synthesized according to

a previously reported procedure.[34] The details of the poly(DMAAm-*co*-NSA) synthesis are provided in the Supporting Information. The M_w, M_n, and M_w/M_n values of the synthesized poly(DMAAm-*co*-NSA) were calculated in the same manner as those of PDMAAm and determined to be 176 kg/mol, 101 kg/mol, and 1.73, respectively. The molar ratio of NSA introduced in the poly(DMAAm-*co*-NSA) was determined to be 0.02 using ^{1}H NMR measurements, according to a previously reported procedure.[34]

Preparation of ZIF-8 NP ion gels. The preparation procedure for the ZIF-8 NP ion gel is as follows. First, a precursor solution of the ZIF-8 NP ion gel was prepared. A certain weight of the ZIF-8 NP suspension in methanol and 4.0 g of [Bmim][Tf_2N] were mixed in a glass vial. Methanol was then evaporated from the mixture at 333 K for 12 h to obtain a ZIF-8 NP suspension in [Bmim][Tf_2N]. Subsequently, 2.5 g of ethanol was added to the suspension to form a new suspension of the ZIF-8 NPs in [Bmim][Tf_2N]/ethanol. Prior to the preparation of the ZIF-8 NP ion gel, the ZIF-8 NP suspension was vigorously agitated *via* vortex mixing for 1 min and ultrasonicated for 20 min to homogeneously disperse the ZIF-8 NPs in the suspension. To the homogeneous suspension, a solution comprising a certain amount of the diamine crosslinker (DGBE) and 3.0 g of ethanol was added, and the suspension was vigorously agitated for 1 min and subsequently degassed under ultrasonication for 1 min. Finally, the degassed suspension was transferred dropwise into a polymer solution comprising a certain amount of poly(DMAAm-*co*-NSA) and 3.0 g of ethanol.

Subsequently, the entire amount of the prepared precursor solution was injected into a closed mold consisting of two glass plates with a fluorinated ethylene propylene (FEP) film and polytetrafluoroethylene (PTFE) spacer (5.0 mm thickness). The dimensions of the mold in which the precursor solution was injected were 80 mm (length) × 80 mm (width) × 5 mm (height). The mold was placed in a thermostat oven maintained at 333 K for 24 h to crosslink poly(DMAAm-*co*-NSA) with DGBE. After 24 h, the top glass plate was removed, and the opened mold was placed in a thermostat oven at 333 K for 24 h to evaporate ethanol from the gel to afford the ZIF-8 NP ion gel. The IL content in the ion gels was 80 wt.%.

We also prepared a single-network (SN) ion gel with a poly(DMAAm-*co*-NSA) network without ZIF-8 NPs. The SN ion gel was composed of 80 wt.% [Bmim][Tf_2N] and 20 wt.% poly(DMAAm-*co*-NSA) crosslinked by DGBE. The SN ion gel was used for comparison while evaluating the mechanical properties of the ZIF-8 NP ion gel. The SN ion gel was prepared in the same manner as the ZIF-8 NP ion gel, except that [Bmim][Tf_2N]/ethanol solution without ZIF-8 NPs was used instead of the suspension of ZIF-8 NPs in [Bmim][Tf_2N]/ethanol solution.

X-ray diffraction (XRD) measurements. The crystalline structures of the ZIF-8 NPs and ZIF-8 NP ion gels were determined using XRD. The XRD patterns were measured using an X-ray diffractometer (D2 PHASER Specifications, Bruker). For the measurement of the crystalline structure of the ZIF-8 NPs, a certain amount of the ZIF-8 NP suspension in methanol was spread in a petri dish and completely dried at 373 K under vacuum. The obtained lumps of dried ZIF-8 NPs were ground using a mortar and pestle. The XRD pattern of the ground ZIF-8 NPs, in the 2θ range of 5 to 30°, was measured. The XRD pattern of the ZIF-8 NP ion gel was directly measured in the 2θ range from 5 to 30°. In both cases, the measurements were conducted at 30 kV and 10 mA using Cu Kα radiation (λ = 1.54 Å).

Evaluation of the mechanical properties of the ZIF-8 NP ion gel. The mechanical properties of the dumbbell-shaped ion gel sample were evaluated using an automatic recording universal testing instrument (EZ-LX, Shimadzu Co.). The thicknesses of the samples were measured using a digital microscope (DMS-300, Leica Microsystems). The length and width of the samples were 17 and 2 mm, respectively. A uniaxial tensile evaluation was performed by stretching the sample at a constant rate of 100 mm/min. The Young's modulus, fracture strain, fracture stress, and fracture energy were measured at least three times for each sample. In the cyclic stretching evaluation, the stretching and returning operations were performed until the breakage of the sample, while incrementally increasing the stretching strain in steps of 0.5 mm/mm. The tearing energies of the ion gels were measured via tearing experiments. The ion gel was cut into a trouser-shape with a length of 75 mm, initial notch of 20 mm, and width of 15 mm. The thickness of the sample was measured using a digital microscope. The ion gel sample was torn by pulling at a constant velocity of 50 mm/min. The tearing energy, which is defined as the energy required to create a unit area of surface fracture in a sample, was calculated by dividing the average force applied during the tearing experiment by the sample thickness.

Swelling evaluation of the poly(DMAAm-co-NSA) network skeleton of the stretched ZIF-8 NP ion gel samples. To evaluate whether the polymer network in the ZIF-8 NP ion gel was destroyed after stretching, a swelling evaluation of the poly(DMAAm-*co*-NSA) network skeleton of the stretched ZIF-8 NP ion gel was conducted. In this study, a ZIF-8 NP ion gel containing 5 wt.% ZIF-8 NPs synthesized at 333 K was used. The thickness of the ion gel was measured using a digital microscope. A dumbbell-shaped specimen of the ion gel possessing a stretching part of length 35 mm and width 4.0 mm was stretched using an automatic recording universal testing instrument at strains of 0, 0.5, 1.5, 2.0, 3.0, and 3.5 mm/mm and then immediately returned to the initial strain. The stretched part of the sample was cut and collected, and ZIF-8 NPs and [Bmim][Tf_2N] were removed from the sample using the following procedure. First, the collected sample was placed in a glass vessel, and approximately 200 g of ethanol was added. The vessel was shaken for 24 h to extract [Bmim][Tf_2N] from the sample. Subsequently, the gel sample without [Bmim][Tf_2N] was immersed in 10 cm^3 of 1 mol/dm^3 HCl aqueous solution for 6 h to dissolve the ZIF-8 NPs. The gel samples were immersed in 200 g ultrapure water for 24 h to form a hydrogel sample with a stretched poly(DMAAm-*co*-NSA) network. The weight of the fully swollen hydrogel sample ($w_{hydrogel}$) was measured. The

hydrogel sample was then dried at 353 K for 3 h, followed by drying at 373 K for 1 h under vacuum to form the dried polymer network skeleton of the stretched ion gel. The weight of the dried polymer network skeleton (w_{dry}) was then measured. The swelling ratio of the stretched poly(DMAAm-*co*-NSA) network in pure water was determined as $(w_{hydrogel} - w_{dry})/w_{dry}$. The swelling ratio of the poly(DMAAm-*co*-NSA) network without stretching was determined in the same manner for comparison.

Evaluation of the mechanical strength recovery of the ZIF-8 NP ion gels. In this study, a ZIF-8 NP ion gel containing 5 wt.% ZIF-8 NPs synthesized at 333 K was used. The thicknesses of the samples were measured using a digital microscope. Using an automatic recording universal testing instrument, a dumbbell-shaped specimen of the ion gel possessing a stretching part of length 17 mm and width 2.0 mm was stretched at a strain of 3.0 mm/mm and immediately returned to the initial strain. The stretched sample was removed from the universal testing instrument and kept in a thermostat oven for a certain period of time. The temperature in the thermostat oven was maintained at 303 or 333 K. After a predetermined time, a uniaxial stretching evaluation of the sample was performed to evaluate the recovery of the mechanical properties.

Conflicts of interest

There are no conflicts to declare.

Acknowledgements

This study was partly supported by KAKENHI (21H01691) from the Japan Society for the Promotion of Science (JSPS).

Notes and references

1. J. F. Wishart, *Energy Environ. Sci.*, 2009, **2**, 956-961.
2. T. Fujimoto and K. Awaga, *Phys. Chem. Chem. Phys.*, 2013, **15**, 8983-9006.
3. M. V. Fedorov and A. A. Kornyshev, *Chem. Rev.*, 2014, **114**, 2978-3036.
4. D. R. MacFarlane, M. Forsyth, P. C. Howlett, M. Kar, S. Passerini, J. M. Pringle, H. Ohno, M. Watanabe, F. Yan, W. Zheng, S. Zhang and J. Zhang, *Nat. Rev. Mater.*, 2016, **1**, 15005.
5. M. Watanabe, M. L. Thomas, S. Zhang, K. Ueno, T. Yasuda and K. Dokko, *Chem. Rev.*, 2017, **117**, 7190-7239.
6. S. Z. Bisri, S. Shimizu, M. Nakano and Y. Iwasa, *Adv. Mater.*, 2017, **29**, 1607054.
7. D. M. Correia, L. C. Fernandes, P. M. Martins, C. Garcia-Astrain, C. M. Costa, J. Reguera and S. Lanceros-Mendez, *Adv. Funct. Mater.*, 2020, **30**, 1909736.
8. X. Han and D. W. Armstrong, *Acc. Chem. Res.*, 2007, **40**, 1079-1086.
9. Y. Liu, J. Chen and D. Li, *Sep. Sci. Technol.*, 2012, **47**, 223-232.
10. Z. Dai, R. D. Noble, D. L. Gin, X. Zhang and L. Deng, *J. Membr. Sci.*, 2016, **497**, 1-20.
11. S. P. M. Ventura, F. A. e. Silva, M. V. Quental, D. Mondal, M. G. Freire and J. A. P. Coutinho, *Chem. Rev.*, 2017, **117**, 6984-7052.
12. Y. Zhao, R. Gani, R. M. Afzal, X. Zhang and S. Zhang, *AIChE J.*, 2017, **63**, 1353-1367.
13. B.-K. Kim, E. J. Lee, Y. Kang and J.-J. Lee, *J. Ind. Eng. Chem.*, 2018, **61**, 388-397.
14. H. Gao, L. Bai, J. Han, B. Yang, S. Zhang and X. Zhang, *Chem. Commun.*, 2018, **54**, 12671-12685.
15. B. Sasikumar, G. Arthanareeswaran and A. F. Ismail, *J. Mol. Liq.*, 2018, **266**, 330-341.
16. Q. R. Sheridan, W. F. Schneider and E. J. Maginn, *Chem. Rev.*, 2018, **118**, 5242-5260.
17. X. Yan, S. Anguille, M. Bendahan and P. Moulin, *Sep. Purif. Technol.*, 2019, **222**, 230-253.
18. A. Noda and M. Watanabe, *Electrochim. Acta*, 2000, **45**, 1265-1270.
19. T. P. Lodge and T. Ueki, *Acc. Chem. Res.*, 2016, **49**, 2107-2114.
20. K. Fujii, H. Asai, T. Ueki, T. Sakai, S. Imaizumi, U.-i. Chung, M. Watanabe and M. Shibayama, *Soft Matter*, 2012, **8**, 1756-1759.
21. K. Hashimoto, K. Fujii, K. Nishi, T. Sakai and M. Shibayama, *Macromolecules*, 2016, **49**, 344-352.
22. Y. Gu, S. Zhang, L. Martinetti, K. H. Lee, L. D. McIntosh, C. D. Frisbie and T. P. Lodge, *J. Am. Chem. Soc.*, 2013, **135**, 9652-9655.
23. F. Moghadam, E. Kamio, A. Yoshizumi and H. Matsuyama, *Chem. Commun.*, 2015, **51**, 13658-13661.
24. F. Moghadam, E. Kamio, T. Yoshioka and H. Matsuyama, *J. Membr. Sci.*, 2017, **530**, 166-175.
25. F. Moghadam, E. Kamio and H. Matsuyama, *J. Membr. Sci.*, 2017, **525**, 290-297.
26. H. Arafune, S. Honma, T. Morinaga, T. Kamijo, M. Miura, H. Furukawa and T. Sato, *Adv. Mater. Interfaces*, 2017, **4**, 1700074.
27. Y. Ding, J. Zhang, L. Chang, X. Zhang, H. Liu and L. Jiang, *Adv. Mater.*, 2017, **29**, 1704253.
28. R. Tamate, K. Hashimoto, T. Horii, M. Hirasawa, X. Li, M. Shibayama and M. Watanabe, *Adv. Mater.*, 2018, **30**, 1802792.
29. T. Ueki, Y. Nakamura, R. Usui, Y. Kitazawa, S. So, T. P. Lodge and M. Watanabe, *Angew. Chem., Int. Ed.*, 2015, **54**, 3018-3022.
30. T. Ueki, R. Usui, Y. Kitazawa, T. P. Lodge and M. Watanabe, *Macromolecules*, 2015, **48**, 5928-5933.
31. D. Weng, F. Xu, X. Li, S. Li, Y. Li and J. Sun, *ACS Appl. Mater. Interfaces*, 2020, **12**, 57477-57485.
32. E. Kamio, T. Yasui, Y. Iida, J. P. Gong and H. Matsuyama, *Adv. Mater.*, 2017, **29**, 1704118.
33. T. Yasui, E. Kamio and H. Matsuyama, *Langmuir*, 2018, **34**, 10622-10633.
34. E. Kamio, M. Kinoshita, T. Yasui, T. P. Lodge and H. Matsuyama, *Macromolecules*, 2020, **53**, 8529-8538.
35. X. Zhao, X. Chen, H. Yuk, S. Lin, X. Liu and G. Parada, *Chem. Rev.*, 2021, **121**, 4309-4372.
36. L. M. Zhang, Y. He, S. Cheng, H. Sheng, K. Dai, W. J. Zheng, M. X. Wang, Z. S. Chen, Y. M. Chen and Z. Suo, *Small*, 2019, **15**, 1804651.
37. M. Zhu, H. Jin, T. Shao, Y. Li, J. Liu, L. Gan and M. Long, *Mater. Des.*, 2020, **192**, 108723.

38. C.-W. Tsai and E. H. G. Langner, *Microporous Mesoporous Mater.*, 2016, **221**, 8-13.
39. S. Wang, C. M. McGuirk, A. d'Aquino, J. A. Mason and C. A. Mirkin, *Adv. Mater.*, 2018, **30**, 1800202.
40. C. R. Marshall, S. A. Staudhammer and C. K. Brozek, *Chem. Sci.*, 2019, **10**, 9396-9408.
41. W. Zhou, H. Wu and T. Yildirim, *J. Am. Chem. Soc.*, 2008, **130**, 15268-15269.
42. S. R. Caskey, A. G. Wong-Foy and A. J. Matzger, *J. Am. Chem. Soc.*, 2008, **130**, 10870-10871.
43. H. Wu, W. Zhou and T. Yildirim, *J. Am. Chem. Soc.*, 2009, **131**, 4995-5000.
44. L. Grajciar, O. Bludsky and P. Nachtigall, *J. Phys. Chem. Lett.*, 2010, **1**, 3354-3359.
45. R. J. Holmberg, T. Burns, S. M. Greer, L. Kobera, S. A. Stoian, I. Korobkov, S. Hill, D. L. Bryce, T. K. Woo and M. Murugesu, *Chem. - Eur. J.*, 2016, **22**, 7711-7715.
46. Y. Maeda, T. Nakamura and I. Ikeda, *Macromolecules*, 2002, **35**, 10172-10177.
47. T. Yasui, S. Fujinami, T. Hoshino, E. Kamio and H. Matsuyama, *Soft Matter*, 2020, **16**, 2363-2370.
48. H. Muta, K. Ishida, E. Tamaki and M. Satoh, *Polymer*, 2001, **43**, 103-110.
49. E. Kamio, T. Yasui, Y. Iida, J. P. Gong and H. Matsuyama, *Adv. Mater.*, 2017, **29**, 1704118.
50. S. Liu, J. Liu, X. Hou, T. Xu, J. Tong, J. Zhang, B. Ye and B. Liu, *Langmuir*, 2018, **34**, 3654-3660.